

STUDY OF STRUCTURAL OPTIMIZATION AND PERFORMANCE ANALYSIS OF MICRO RING RESONATOR AS OPTICAL RANDOM ACCESS MEMORY

THESIS REPORT

*Submitted in partial fulfillment of the requirements for the award of the
Degree of Master of Technology in Electronics and Communication
Engineering with specialization in Communication Systems by the
A P J Abdul Kalam Technological University*

by

SHYAMA M. S.

Reg. No. TKM21ECCS11



DEPARTMENT OF ELECTRONICS AND COMMUNICATION
ENGINEERING

TKM COLLEGE OF ENGINEERING

KOLLAM 691 005

MAY 2023

STUDY OF STRUCTURAL OPTIMIZATION AND PERFORMANCE ANALYSIS OF MICRO RING RESONATOR AS OPTICAL RANDOM ACCESS MEMORY

THESIS REPORT

*Submitted in partial fulfillment of the requirements for the award of the
Degree of Master of Technology in Electronics and Communication
Engineering with specialization in Communication Systems by the
A P J Abdul Kalam Technological University*

by

SHYAMA M. S.

Reg. No. TKM21ECCS11



DEPARTMENT OF ELECTRONICS AND COMMUNICATION
ENGINEERING

TKM COLLEGE OF ENGINEERING

KOLLAM 691 005

MAY 2023

DEPARTMENT OF ELECTRONICS & COMMUNICATION
ENGINEERING

TKM COLLEGE OF ENGINEERING

KOLLAM 691 005



CERTIFICATE

Certified that this Project report titled “**STUDY OF STRUCTURAL OPTIMIZATION AND PERFORMANCE ANALYSIS OF MICRO RING RESONATOR AS OPTICAL RANDOM ACCESS MEMORY**” is a bonafide record of the work done by **SHYAMA M. S.** (Reg. No.TKM21ECCS11) under my supervision, in partial fulfillment of the requirements for the award of the Degree of Master of Technology in Electronics and Communication Engineering with specialization in Communication Systems by the A P J Abdul Kalam Technological University.

Coordinator & Guide

Dr. NISHANTH N.

Professor

Dept. of ECE, TKMCE

External Guide

Dr. SOORAJ R.

Associate Professor

Dept. of Avionics, IIST

HoD

Prof. SHABEER S.

Head, Dept. of ECE

Dept. of ECE, TKMCE

Acknowledgement

At the outset, I consider it my duty to thank Almighty God for giving me the necessary wisdom to successfully complete this project presentation.

I express my sincere gratitude and thanks to **Dr. T. A. SHAHUL HAMEED**, Principal, TKM College of Engineering for his encouragement and support.

I thank **Prof. SHABEER S.**, HOD, Department of Electronics and Communication, for his encouragement and support.

I express my sincere thanks and heart full gratitude to our PG coordinator and guide, **Dr. NISHANTH N.**, Professor, Department of Electronics and Communication Engineering, for the support and encouragement during the course of this project work.

I take this opportunity to express my sincere gratitude and profound thanks to my external guide, **Dr. SOORAJ R.**, Associate Professor, Department of Avionics, IIST Thiruvananthapuram for his advice, supervision and patience during the course of project preparation and presentation and for providing me guidance and critical inputs in the preparation and presentation of my project.

I would also like to express my sincere gratitude to all my teachers, friends, parents, spouse, son and daughter for their much needed support during the course of project work.

SHYAMA M. S.

TKM21ECCS11

ABSTRACT

This study investigates the performance of high quality optical resonator which act as memory cells to store data bits. The theoretical performance thresholds of optical resonator memory cells for use in optical RAM are examined in this research. This work includes the literature survey of optical Micro ring resonator based previous studies. This work mainly focuses on increasing the memory capacity of micro ring resonator structure and how the structural differences affects the performance.

For that, various structures are simulated and examined. Besides looking at the storage time, we also examined the power that was received at the output. Taking into account light's output power, how long it lasts inside a structure and the size of the structure, this work suggests a few micro ring resonator designs that can function as optical memories.

Contents

| | |
|--|-----------|
| List of Figures | v |
| List of Tables | vi |
| 1 Introduction | 1 |
| 1.1 Micro Ring Resonator | 2 |
| 1.1.1 Principle of operation of micro-ring resonator | 4 |
| 2 Literature Review | 5 |
| 3 Methodology | 9 |
| 3.1 Ansys Lumerical Software | 9 |
| 3.2 Design of single ring resonator | 10 |
| 3.2.1 Total length of the ring | 11 |
| 3.2.2 Gap and the length of the coupler segment | 12 |
| 4 Results and Discussion | 14 |
| 4.1 Simulation and Analysis | 14 |
| 4.1.0.1 Theoretical calculation of Storage time | 16 |
| 4.1.1 Parallel cascading of rings and simulation results | 17 |
| 4.1.1.1 Two ring structure | 17 |
| 4.1.1.2 Three ring structure | 18 |
| 4.1.1.3 Four ring structure | 19 |
| 4.1.1.4 Interconnected ring structure | 20 |
| 4.1.1.5 Embedded ring structure | 21 |
| 4.1.2 Comparison of performances of different structures | 21 |

| | | |
|----------|--|-----------|
| 4.1.2.1 | Comparison between single ring and Embedded ring | 22 |
| 4.1.2.2 | Comparison between Four ring structure and interconnected ring structure | 23 |
| 5 | Conclusion and Future scope | 25 |
| | References | 28 |

List of Figures

| | | |
|------|---|----|
| 1.1 | Micro ring resonator | 3 |
| 2.1 | An structure with two embedded microrings | 6 |
| 2.2 | Schematic of dual-concentric MRR | 7 |
| 2.3 | N-bit all-optical digital-to-analog converter | 8 |
| 2.4 | An embodiment of optical ring-resonator RAM | 8 |
| 3.1 | Group Index | 11 |
| 3.2 | Design parameters of optical ring resonator | 12 |
| 4.1 | Features of the source | 14 |
| 4.2 | Frequency spectrum at the drop port | 15 |
| 4.3 | Signal between the waveguides using one ring | 15 |
| 4.4 | Effective refractive index of single ring resonator | 16 |
| 4.5 | Two ring structure | 17 |
| 4.6 | Signal between the waveguides using two rings | 17 |
| 4.7 | Three ring structure | 18 |
| 4.8 | Signal between the waveguides using three rings | 18 |
| 4.9 | Four ring structure | 19 |
| 4.10 | Signal between the waveguides using four rings | 19 |
| 4.11 | Interconnected ring structure | 20 |
| 4.12 | Signal between the waveguides using interconnected ring structure | 20 |
| 4.13 | Embedded ring structure | 21 |
| 4.14 | Signal between the waveguides using embedded ring structure | 21 |
| 4.15 | Power at the output port of single ring resonator | 22 |
| 4.16 | Power at the output port of embedded ring structure | 23 |

| | |
|---|----|
| 4.17 Power at the output port of four ring structure | 23 |
| 4.18 Power at the output port of interconnected structure | 23 |

List of Tables

| | | |
|-----|---|----|
| 3.1 | Parameters of Micro ring resonator | 12 |
| 4.1 | Retention time corresponding to the structures with different number of rings | 22 |
| 4.2 | Storage time and Power corresponding to the structures with different number of rings | 24 |

Chapter 1

Introduction

Over the past few decades, the expansion of internet communications has been driven by fibre optic technology, enabling the transmission of enormous volumes of information quickly with less delay. There are concerns that bandwidth restrictions and internet latency will impede the development of real-time applications, particularly for what is frequently referred to as the internet of things. The latency associated with optic-to-electronic conversion at network nodes can be reduced by maintaining the signal in the optical domain, which is one proposed way for increasing internet speeds.

In the research of maintaining the signal in the optical domain, we came across different devices which can store light. The absence of an optical random-access memory (RAM) technology that can store and retrieve data at multigigabit-per-second bit rates has long troubled optical experts. Using optical fibre delay lines, one method of high-speed optical buffering stores a train of high-bit-rate pulses as travelling waves. Unfortunately, delay lines frequently have a small capacity and are clumsy. The size of delay lines might be decreased because to developments in low-loss planar waveguide (WG) circuits and slow light techniques in photonic crystals. The capacity of slow light delay lines is, however, restricted to fewer than roughly 1000 bits due to losses in slow light WGs (including PC WGs and other planar circuits).

Optical resonators, which store the energy of individual data pulses, are a potential replacement for delay line buffers [1]. The time-dependent management of the coupling medium, which ensures that the maximum amount of energy is captured in the cell and that the energy is released when needed, is essential to this form of

resonator memory cell. High Q resonators can trap energy for a nanosecond or more. However, the theoretical potential and limitations of resonator memory cells have not been fully explored.

Photon's basic nature prevents its spatial confinement, therefore "storing light" has come to be rather debatable during the previous few decades. The first optical memory was documented in 1965 using a folded optical delay line [2], and many research efforts in establishing optical memory capability began as an interesting scientific exercise. Twenty years later, in 1985, the first optical flip-flop (SR-FF) mechanism was introduced [3], and for the following few years, research efforts were mostly directed toward momentarily containing light inside a medium, in the form of a continuous loop. Different types of schemes, including optical delay lines, slow light optical buffers, as well as more recently, all-optical flip flop devices, were introduced for the purpose of resolving packet-level contention as fibre optics gradually became a widely used telecommunication transmission platforms. This increased research interest in optical memories.

1.1 Micro Ring Resonator

The use of optical micro resonators as the essential building blocks for a range of photonics applications has shown significant potential. Micro ring resonator can be used in a wide variety of devices, including lasers, amplifiers, sensors, switches, routers, optical add/drop (de)multiplexers (OADMs), optical channel dropping filters (OCDs), and artificial media. We generalise the word "microring resonators" and specialise the term "microresonators" for the sake of clarity and in keeping with how they are currently used in the literature in this field. These phrases are used interchangeably to refer to different type of compact geometries that enable cyclically propagating modes to close in on themselves. A waveguide that transmits light in a closed loop constitutes one particular implementation of a microring resonator. But generally speaking, the loop can be any closed shape, such a disc, a racetrack, or an ellipse. The micro resonator in the instance of a ring is just a curved waveguide that is closed in on itself to create a cavity that is resonant and can support both transverse and longitudinal modes. But in this closed geometry, there is no need for an inner

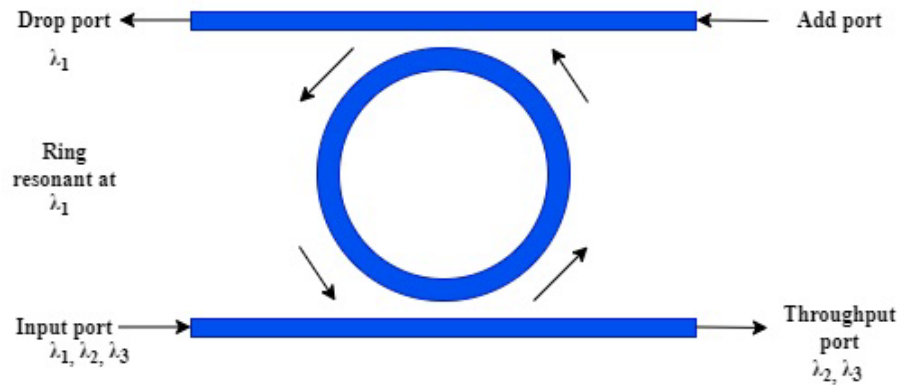


Figure 1.1: Micro ring resonator

dielectric border to contain and conduct light. The presence of "whispering gallery" modes in a micro disc or microsphere resonator serves as proof of this. Access to the resonant cavity's modes is made possible by positioning a micro resonator close to one or two waveguide Figure 1.1.

In this particular configuration, a phenomenon similar to tunnelling in solid-state physics (evanescent coupling) is used to access the resonant modes. When an optical signal is channelled in a waveguide, its component wavelengths are resonant with the cavity if the cavity's (effective) circumference can accommodate an integer number of wavelengths. An enhanced circulation of intensity can accumulate inside the resonator for these specific spectral components of the signal. The ability to extract the resonant, circulating signal is made possible by the presence of an another waveguide attached to the ring. Wavelengths of the component that do not resonant with the ring completely bypass it. Microring resonators function as an energy density temporary compressor and spectral filter at their most basic level. These characteristics do not only apply to microring resonators.

Microring resonators have several advantages over Fabry- Perots despite having a similar functional design. Firstly, due to their planar design, monolithic microfabrication techniques are naturally compatible with them. Second, high finesse operation can be accomplished by widening the spacing between evanescent couplers rather of using multilayer or distributed Bragg reflectors. Thirdly, the need for pricey Faraday circulators is eliminated because the identical waves that is transmitted and reflected waves occupy spatially different channels. Fourth, due to the same reasoning, three completely new, qualitatively distinct conceivable configurations for arrays of res-

onators are made possible, despite the fact that there is only one common way to sequence Fabry-Perot arrays.

Two of the many benefits of the small size of microresonators currently made possible by cutting-edge fabrication techniques are highlighted here. First, high bandwidths (GHz to THz) are generally possible because the propagation velocity of light is on the scale of a few hundred micro meter per pico seconds in the majority of optical materials of interest. Second, their diminutive size enables the integration of numerous devices on a single chip, opening the door to previously unattainable high-level features like rapid alloptical data processing. These intrinsic benefits may make optical microresonators necessary for very large-scale integration (VLSI) of high-bandwidth photonics.

1.1.1 Principle of operation of micro-ring resonator

Figure 1.1 shows a basic micro ring resonator with two straight wave guide and one ring wave guide. The input light is given through the input port. Only the wavelength which satisfies the resonant condition will couple into the ring. One of the resonant wavelengths of light couples into the ring and is then downloaded from the drop port when light of a specific wavelength couples through the input port. This is known as the MRR's ON state. If not, the through port will display the maximum, also known as the MRR's OFF status. The resonant condition is given by the Equation 1.1

$$m\lambda_{res} = 2\pi r n_{eff} \quad (1.1)$$

Where m is the mode number of the ring resonator, λ_{res} is the resonance wavelength, n_{eff} is the effective refractive index of the waveguide mode, and r is the radius of the ring.

Energy inside a structure can be treated as storing information or it can be called as a memory. The main aim of this work is to find out the ways to increase the storing time of light inside the ring without losing much power. Different structures are designed and simulated for this purpose.

Chapter 2

Literature Review

Due to its benefits of very small size, high integration, and low cost silicon photonics has emerged as an appealing and promising solution in response to the demand for next generation communication and large-scale computing, such as big data, cloud computing, the Internet of Things, artificial intelligence, and so forth. One of the most important research tools in use today is the photonic microring resonator. By cascading the ring modulators in sequence, it may produce higher order optical filters, and it is also utilised in bio sensing to describe various absorption spectra for the purpose of chemical identification. Basic silicon waveguide components have applications in sensors, filters, wavelength converters, digital to analog converters, optical routers, optical logic gates and so on. In this section we examine the previous works.

Kui et al., [4] demonstrated the analysis of photonic micro ring resonator according to its resonance response. In this study the resonance response analysis of a photonic microring resonator is presented. The FWHM and Q-factor, two parameters for the study, have also been mathematically calculated. Three ring parameters, including the coupling coefficient, waveguide material group index, and ring radius, have also been examined in terms of their effects on ring resonance at various modulation voltages. Increasing the ring radius, they obtained a higher quality factor (Q-factor). The rise in resonance Q-factor can be seen in the lower value of the ring coupling coefficient. Additionally, the resonance quality has been shown to rise with the greater waveguide material group index.

W. Hong et al., [5] presented a microring resonator with two embedded microring and studied theoretically. This work presents and conceptually investigates a micror-

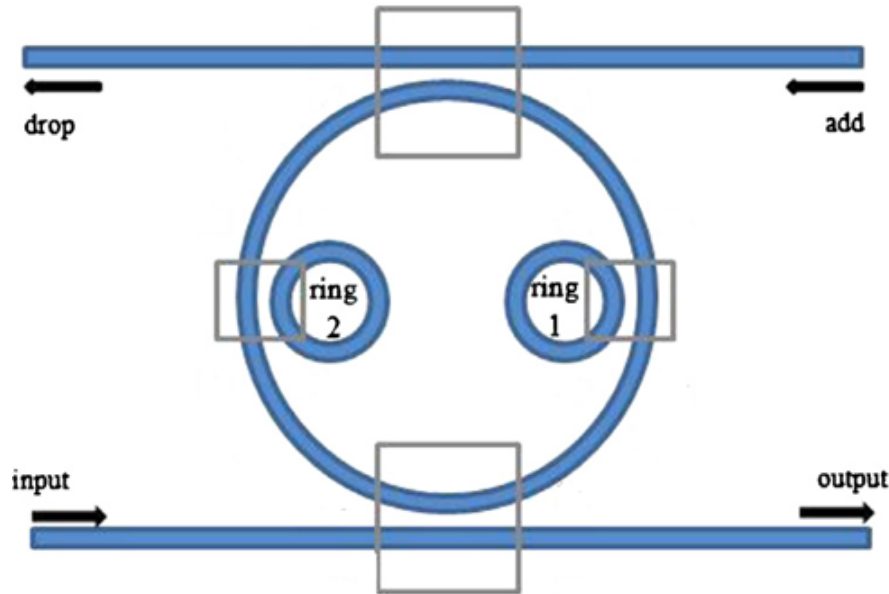


Figure 2.1: An structure with two embedded microrings

ing resonator with two embedded microrings (MRTEM). To simulate structure and examine the relationships between add and drop spectrum and embedded microring configurations, the transfer matrix method (TMM) was used. By using TMM, three different embedded microring arrangement types have been proposed and examined. Theoretical and simulation results demonstrate that our construction has a higher Q factor than a conventional microring structure and that the MRTEM spectrum is independent of embedded configurations. Figure 2.1 shows the proposed structure.

Y. Xu et al., [6] suggested a mathematical model for high- Q silicon dual-concentric MRR. The coupled mode theory has been used in this study to explore the dual-concentric Micro ring resonator and racetrack resonator made of high-Q silicon. The resonance splitting phenomena is described and alleviated by the theoretical model. For the creation of dualconcentric MRR and racetrack resonators, CMOS manufacturing is used. The study demonstrates that the waveguide width and distance between the inner and outer rings can be changed to modify the asymmetry of resonance splitting. Figure 2.2 shows the schematic of dual concentric ring resonator.

Many works related to the application of Micro ring resonator are going on. Addya, S et al., [7] demonstrated a temperature sensor using Optical ring resonator. In this study, a temperature sensor based on an optical ring resonator has been demonstrated using silicon and germanium as its materials. It was accomplished using a

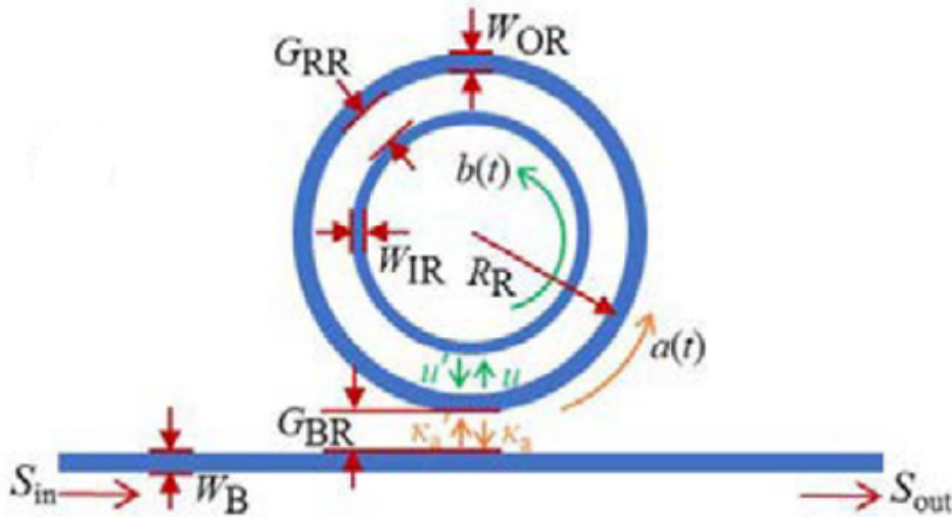


Figure 2.2: Schematic of dual-concentric MRR

Z-domain optical delay line signal processing approach. These sensors can measure the temperature between room temperature to high temperature of around 530oC. The temperature ranges of a silicon (Si) fiberbased optical sensor is between 30oC and 500oC, while that of a germanium (Ge) fiber-based sensor is between -25 oC and 300oC. Ge and Si-fibers have obtained temperature sensitivities of 5.55 and 2.97MHz/C, respectively.

Mamdouh, T. et al., [8] suggested a new design for a ring resonator tunable optical filter. In this study, a brandnew design for a tunable optical filter with a ring resonator is put forth. A directional coupler connects two rings in this architecture, and tuning is accomplished by controlling the distance between the coupler's two parallel guides via a micro-electromechanical systems (MEMS) actuator. The suggested construction enables mechanical tweaking of the resonance frequency in the C- band throughout a 13.4 nm spectral breadth.

Rakshit et al., [11] suggested a structure based on micro ring resonator that can be used as an All-optical N-bit digital-toanalog converter and 1×2 optical splitters. That structure can convert N-bit digital optical signal to an analog optical signal. This study proposed and described an all-optical N-bit digitalto-analog converter that converts N-bit optical digital signals into optical analogue signals using microring resonators and 1×2 optical splitters. They created and simulated a two MRR, two-one-two optical splitter, two-bit digital-to-analog converter. The two operands of

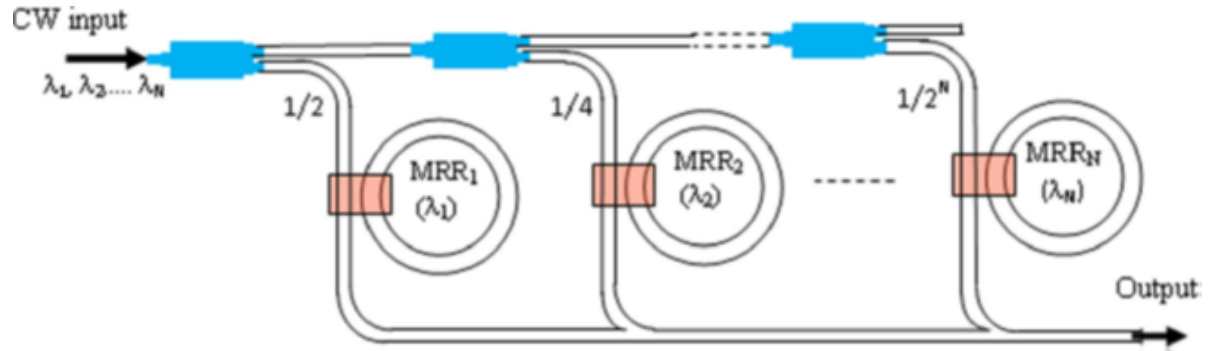


Figure 2.3: N-bit all-optical digital-to-analog converter

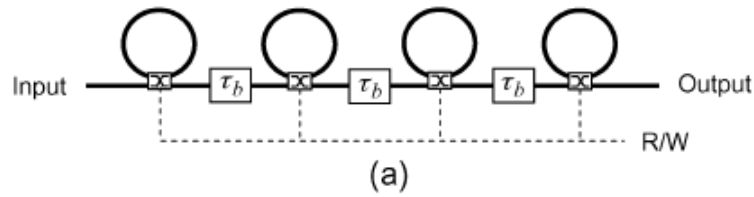


Figure 2.4: An embodiment of optical ring-resonator RAM

the logical operations used to modulate the two MRRs are represented by two optical pump signals. High extinction ratios of 16.94 and 15.98 dB are achieved by the suggested silicon MRRs at very low pump powers of 1.76 and 1.82 mW, respectively. Figure 2.3 shows N-bit all-optical digital-to-analog converter.

S. Tucker et al., [18] examines the properties of optical resonator memory cells, in which a data is stored in an optical resonator. This study investigates the characteristics of high-optical resonator memory cells, which store data bits. It is demonstrated that losses in the resonators, the extinction ratio and chirp of the variable coupling medium, as well as chirp on the input signal, are the factors that eventually restrict resonator-based optical memory. They suggested that it is feasible to couple a specific wavelength which can be considered as data from an incoming light signal into the ring resonator and store energy by carefully optimising the values of the coupling coefficient of the ring-resonator coupler as a function of time. The coupling coefficient can then be adjusted one more to read out the pulse energy afterwards. Figure 2.4 shows an embodiment of optical ring-resonator RAM.

Chapter 3

Methodology

This work mainly focused to simulate different structures of micro ring resonators to find out a suitable structure which will store the light inside for a longer time. For that first we designed a single ring resonator which couple the light from the input port into it efficiently. Then we simulated different structures and analysed its performance. For the simulation purpose we use Ansys Lumerical software.

3.1 Ansys Lumerical Software

The design of photonics parts, circuits, and systems is made possible by the comprehensive photonics simulation software suite Ansys Lumerical. Designers can model interacting optical, electrical, and thermal effects thanks to tools that seamlessly integrate device and system level functionality. A variety of processes that combine device multiphysics and photonic circuit simulation with external design automation and productivity tools are made possible by flexible interoperability between products. The top foundries in the sector can be supported by automation and workflows based on Python for creating and utilising compact models.

Here we used FDTD (Finite Difference Time Domain) method for simulation purpose. This well designed FDTD method implementation offers best solver performance across a wide range of applications. The integrated design environment offers advanced post-processing, optimisation, and scripting capabilities, allowing us to concentrate on our design while leaving the rest to us.

Any structure where the required physics are described by Maxwell's equations can

be simulated using FDTD. LEDs, solar cells, filters, optical switches, semiconductor-based photonic devices, sensors, nano- and micro-lithography, nonlinear devices, and meta-materials are examples of typical uses for this technique.

Modelling nano-scale optical devices can be done with precision and power using the Finite-Difference Time-Domain (FDTD) approach. Without using any physical approximations, FDTD directly solves Maxwell's equations, and the scale of the largest issue is only constrained by the amount of computing power available. Maxwell's equations are solved using the FDTD method on a mesh, and E and H are calculated at grid locations separated by Δx , Δy , and Δz , with E and H interlaced in all three spatial dimensions. The effects of scattering, transmission, reflection, absorption, etc. are all included in FDTD. Although the Fast Fourier Transform (FFT) and Discrete Fourier Transform (DFT) are used for frequency analysis, the FDTD is a time-domain approach.

3.2 Design of single ring resonator

We want to design a micro ring resonator which will couple only the wavelength 1550 nm. We select this wavelength because when considering high index contrast waveguides, the bending losses and propagation losses are small at this wavelength. In this work we neglect all losses, but different losses can be considered for future work.

We use a ring shaped waveguide and two straight waveguides. The dropped power at the drop port is

$$P_D = P_{IN} \frac{|t_{12}|^4}{|1 - t_{11}^2 \exp^{i\beta L}|^2} \quad (3.1)$$

On resonance state, after one round trip time, the phase acquired by the signal is an integer multiple of 2π

$$\beta L = 2\pi N \quad (3.2)$$

where N is the mode number. Ring length is an integer multiple of the effective wavelength if the effective refractive index is wavelength independent on resonance. In fact, the free spectral range(FSR) separates the resonances and the effective index

depends on wavelength. Let n_g is the group index and Q is the Q factor, then

$$FSR = \frac{\lambda^2}{n_g L} \quad (3.3)$$

$$n_g = c \frac{d\beta}{d\omega} \quad (3.4)$$

$$Q = \frac{\lambda}{2\delta\lambda} = \frac{n_g L \pi}{\lambda} \frac{|t_{11}|}{1 - |t_{12}|^2} \quad (3.5)$$

Using the above equations, a ring resonator is designed. It can be used for a WDM system. Normally WDM systems are with channel spacing of 200GHz. For getting output at every 16th channel, the FSR should be 3200GHz. Also we would like to have 100GHz FWHM of the drop, so the Q factor should be approximately 2000. The waveguide is made of SOI. The width of waveguide is 400 nm and height is 180 nm.

3.2.1 Total length of the ring

We computed the group index from 1500 nm to 1600 nm using the Eigenmode Solver on the cross section of a 3D waveguide. Around 1550 nm, we can see that the group index is roughly 4.63. Figure 3.1 shows the result. This exceeds the effective

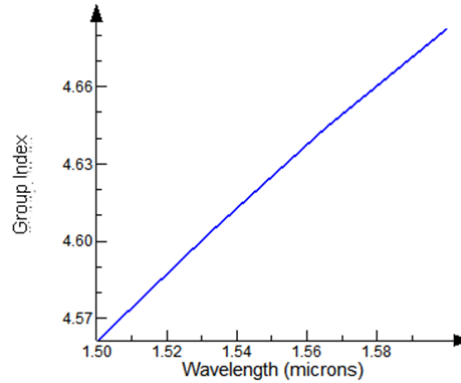


Figure 3.1: Group Index

index at this wavelength by a substantial margin.

$$\text{Group index, } n_g = 4.63$$

$$\text{Length of the ring, } L = \frac{c}{n_g FSR} \simeq 20.2 \mu\text{m}$$

$$\text{Radius of the ring, } R = 3.2 \mu\text{m}$$

3.2.2 Gap and the length of the coupler segment

We calculated the coupling coefficient values using the Q factor values.

$$t_{11} = \sqrt{\left(\frac{n_g L \pi}{2Q\lambda}\right)^2 + 1} \frac{n_g L \pi}{2Q\lambda} \simeq 0.95$$

$$t_{12} = \sqrt{1 - t_{11}^2} \simeq 0.31$$

The coupling length is calculated using the equation(8). Here Δn is the difference in the effective refractive index of the anti symmetric and symmetric coupled mode.

$$L_{\text{coupler}} = \frac{\lambda}{\pi \Delta n} \sin^{-1}(|t_{11}|)$$

We used Lumerical FDE Eigenmode Solver to calculate the index of the coupled waveguide system.

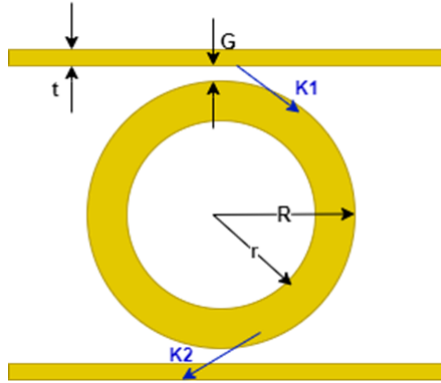


Figure 3.2: Design parameters of optical ring resonator

Table 3.1: Parameters of Micro ring resonator

| Parameter | Values(micro meter) |
|--------------------------------|---------------------|
| Thickness of the waveguide, t | 0.4 |
| Coupling Gap, G | 0.1 |
| Outer ring radius, R | 3.4 |
| Inner ring radius, r | 3 |
| Coupling coefficient, t_{11} | 0.95 |
| Coupling coefficient, t_{12} | 0.31 |

It is obtained that $\Delta n = 0.109$ at 1550 nm using a 100 nm gap between the waveguides. This results in a coupling length of roughly 1427 nm. In practise, we'll utilise a coupling length of zero, and the bent portion of the ring close to the straight

waveguide will provide enough coupling. The structure and the design parameters are explained in the Figure 3.2 and Table 3.1.

Chapter 4

Results and Discussion

4.1 Simulation and Analysis

Here we took a micro ring resonator made of silicon material with parameters as shown in the Table 3.1. The ring shaped waveguide is made on a SiO_2 substrate layer. The substrate layer has $4 \mu m$ thickness. That results in fundamental TE mode. The simulation is done using Ansys Lumerical software. Lumerical MODE finite difference solver is used for obtaining the results.

The source applied to the upper straight waveguide. Source contains the spectrum from 1500 nm to 1600 nm. Features of the source are given in the Figure 4.1.

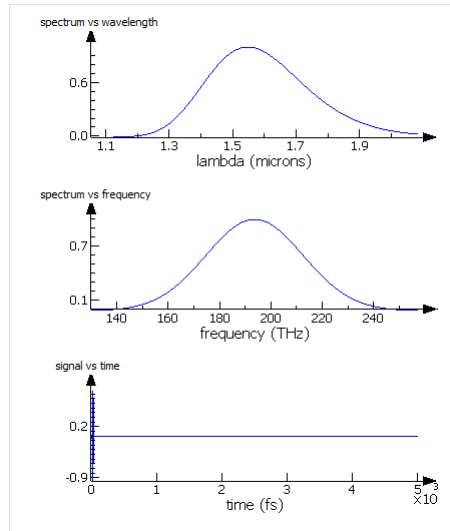


Figure 4.1: Features of the source

Since we designed to couple only the wavelength 1550 nm, only that wavelength

is coupled into the ring. The coupled wavelength can be dropped out through the drop port at the lower straight waveguide and then we calculate the time that the wavelength is inside the ring.

After simulation , when we check the frequency spectrum at the output port which is in the lower waveguide we got that spectrum is at 1550 nm. So from that it is clear that only the wavelength which is coupled into the ring and drop port is 1550 nm. All other wavelengths are transmitted through the throughput port. The Figure 4.2 shows the frequency spectrum at the drop port.

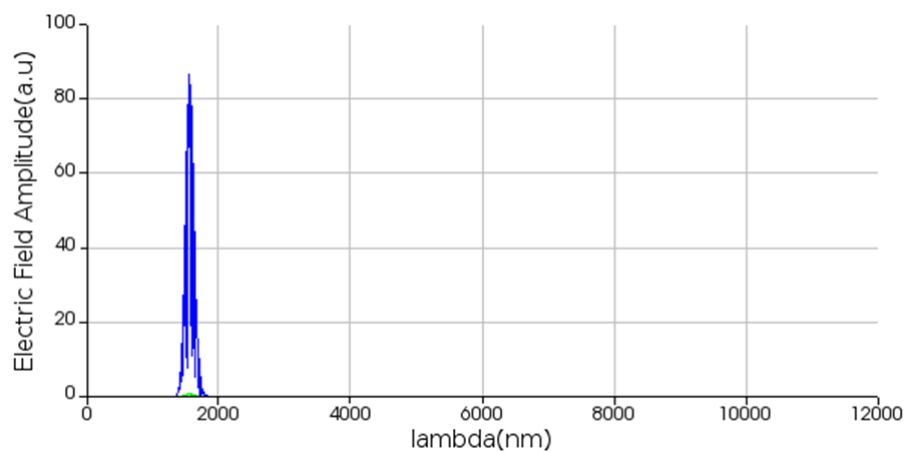


Figure 4.2: Frequency spectrum at the drop port

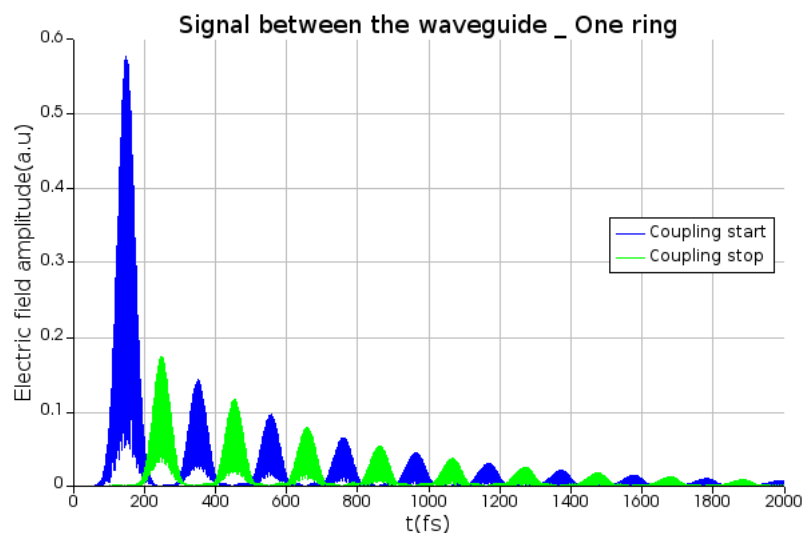


Figure 4.3: Signal between the waveguides using one ring

The time period can be calculated using the Time monitor. By taking the difference between the arrival of the wavelength from the upper waveguide to the lower

waveguide we can calculate the time that the wavelength is inside the ring.

Figure 4.3 shows the signal at both upper and lower waveguides. It is obvious from that the coupling starts at 150 fs and the light reaches at the lower waveguide at 250 fs. That is between this time period the light is inside the ring. By taking the difference we calculated the time period of the wave inside the ring, it is 100 fs. We got signal at the lower waveguide about 2000 fs, but the power reduces gradually. A detectable signal is at 250 fs. So using one ring we can store the data inside the resonator structure for 100 fs.

4.1.0.1 Theoretical calculation of Storage time

Optical path length is related to radius of the ring and effective refractive index. The relationship can be expressed in the equation. Effective refractive index is 2.2 . It is shown in the Figure 4.4

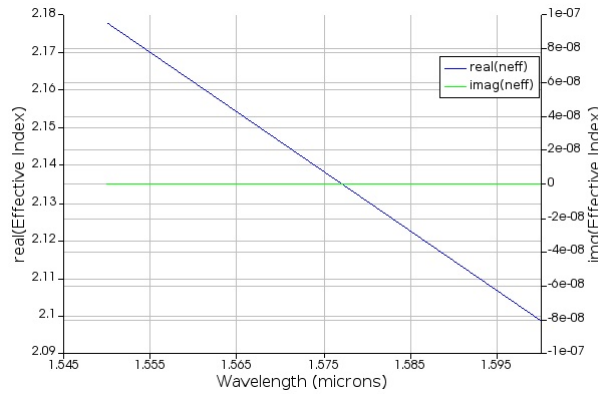


Figure 4.4: Effective refractive index of single ring resonator

$$\begin{aligned}
 \text{Optical path Length, } L &= \pi r n_{eff} \\
 &= \pi \times 3.4 \times 10^{-6} \times 2.2 \\
 &= 2.35 \times 10^{-5} m \\
 \text{Velocity of Light, } V &= 3 \times 10^8 m/s \\
 \text{Time period} &= \frac{L}{V} \\
 &= 78 fs
 \end{aligned} \tag{4.1}$$

There is almost 22 fs difference between theoretical and calculated value.

4.1.1 Parallel cascading of rings and simulation results

The main focus of this work is how to improve the storage time of the wave inside the structure. So from previous work it is found out that as the number of rings increases the time period also increases. So here simulated some structures and analysed the time period.

4.1.1.1 Two ring structure

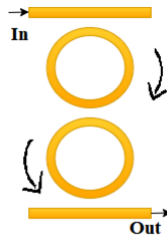


Figure 4.5: Two ring structure

In this structure, the two rings are cascaded parallelly. The input enters from the input port to the first ring through coupling between the straight waveguide and ring waveguide. Then it is again coupled to the second ring from the first and then to the lower straight waveguide and to the output port.

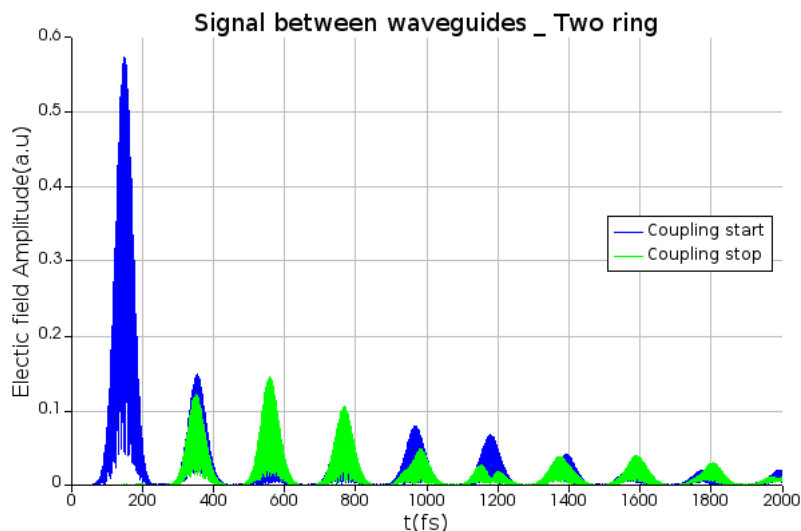


Figure 4.6: Signal between the waveguides using two rings

From Figure 4.6 we can see that coupling to the ring starts at 150 fs and the peak power received at 550 fs. So by taking the difference we can say that the light is inside

the ring structure for 400 fs. But the obvious difference using the two rings compared to one ring is that the power is not reducing gradually. The peak power is observed at second round trip. Also from 345 fs to 765 fs the power had retained without much reduction that is at the output port we get almost same power for 420 fs.

4.1.1.2 Three ring structure

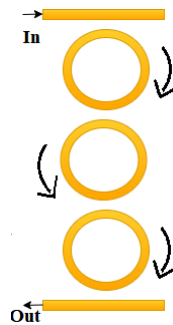


Figure 4.7: Three ring structure

In this three ring structure, the light is coupled to the first ring and second ring and the to the third. From the third ring the light is coupled to the lower waveguide.

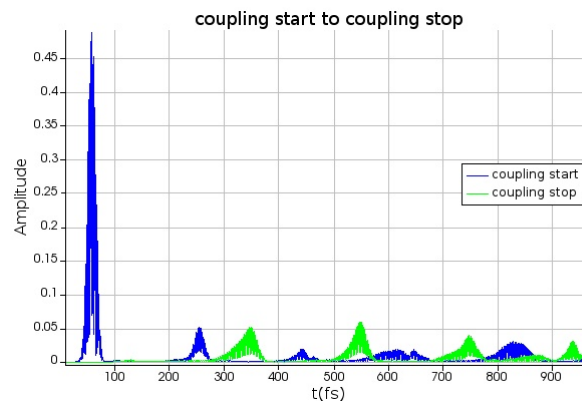


Figure 4.8: Signal between the waveguides using three rings

From Figure 4.8 it is seen that the light enters into the ring structure at 140 fs and signal with high power obtained at 630 fs. So the light is inside the for 490 fs. Also reduced power is obtained at lower straight waveguide. But the power received at the output port maintained for 410 fs, which is almost same in case of two ring structure.

4.1.1.3 Four ring structure

In this structure we used four rings which are parallel coupled. In all the structures we used identical rings. Main observation from these structures is that the light coupled from one ring to another to the opposite sides.

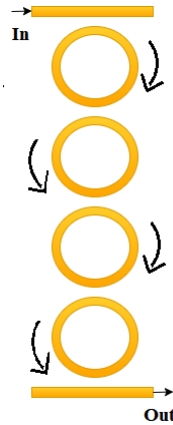


Figure 4.9: Four ring structure

From Figure 4.10 it is seen that the light enters into the ring structure at 140 fs and signal with high power obtained at lower straight waveguide at 930 fs. So the light is inside the for 790 fs. Also very low power is obtained at lower straight waveguide. But the power received at the output port maintained only for 200 fs, which is very low compared to other structures.

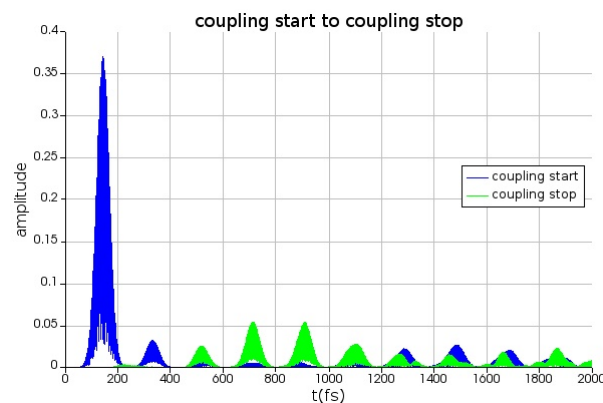


Figure 4.10: Signal between the waveguides using four rings

So from this understood that more number of rings cascading vertically increases the storage time of light inside the ring structure but reduction in power also happens as the number of rings increases. So adding more number of rings will not be a good

decision. So we introduced some structural changes in this four ring structure and analysed its performance.

4.1.1.4 Interconnected ring structure

In this we introduced coupling rather from one ring to another than an interconnected coupling between the ring. So the input light is coupled to the first ring from the upper straight waveguide and then it is coupled to two rings. Then the light from these two rings coupled to a fourth ring and then to lower straight waveguide. The Figure 4.11 explains the structure and the passage of light.

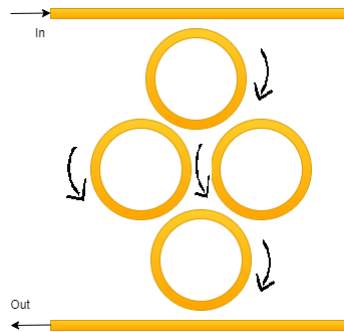


Figure 4.11: Interconnected ring structure

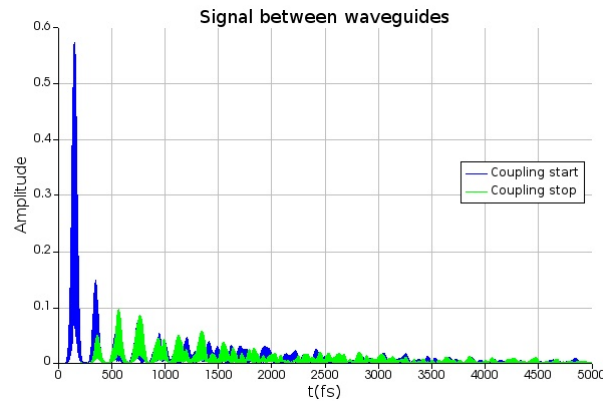


Figure 4.12: Signal between the waveguides using interconnected ring structure

From Figure 4.12 it is clear that the light enters to the structure at 150 fs and maximum power received at the lower waveguide at 565 fs. So the light is inside the structure for 415 fs. That is less compared to four rings coupled vertically. But a large difference is seen in case of power. Compared to vertical coupling more power is obtained for this structure. Also a detectable power is retained in the output port for

640 fs. That is a great achievement. So this structure is useful for storing light compared to other structures.

4.1.1.5 Embedded ring structure

Although we see that interconnected structures are more capable of storing light, In order to reduce the size of overall structure, we simulated embedded structure and analysed its performance. Figure 4.13 shows the simulated embedded structure.

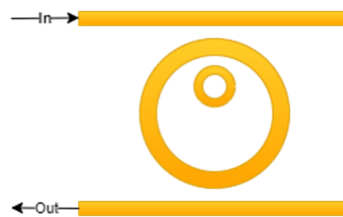
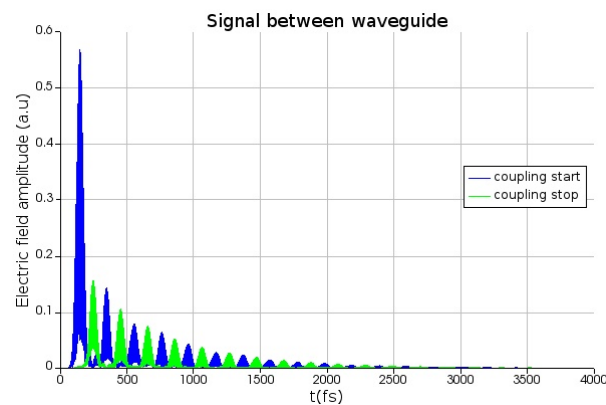


Figure 4.13: Embedded ring structure

Figure 4.14 shows the simulated output. From that it is clear that light enters to 150 fs to the bigger ring from the upper straight waveguide and then a part of light is again coupled into the smaller ring. So maximum power obtained at 250 fs as we seen in case of one ring structure. But the obvious difference is seen at power level. So we find out that embedded rings can be used for increasing the power level of the light inside the ring structure.



4.13

Figure 4.14: Signal between the waveguides using embedded ring structure

4.1.2 Comparison of performances of different structures

First we compare the retention time of the four structures from one ring to four rings which are parallel coupled. The Table 4.1 shows the time period of light inside

Table 4.1: Retention time corresponding to the structures with different number of rings

| No.of rings | Retention time (fs) |
|-------------|---------------------|
| One ring | 100 |
| Two ring | 400 |
| Three ring | 490 |
| Four ring | 790 |

the structure for different structures.

From Table 4.1 we can see that as the number of rings increases the storage time also increases, but it is not linear increase.

4.1.2.1 Comparison between single ring and Embedded ring

The Figure 4.15 and Figure 4.16 shows the power level of the two structures. From that figures it is clear that when using single ring we got only maximum 0.25 milli watt power but if we use embedded ring it will become 0.3 milli watt. Also the spectral width is high for embedded structures. The Figure 4.17 and Figure 4.18 shows the

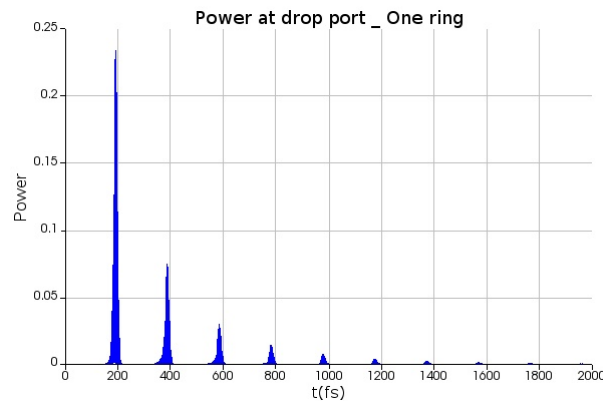


Figure 4.15: Power at the output port of single ring resonator

power level of the two structures. In the case of four ring structure the power has low value in the range of micro watts at its maximum value. Also it reduces to zero range after 1500 fs. But in the case of interconnected structure the peak power value is in the range of milli watts and it reduces to zero only after 2000 fs.

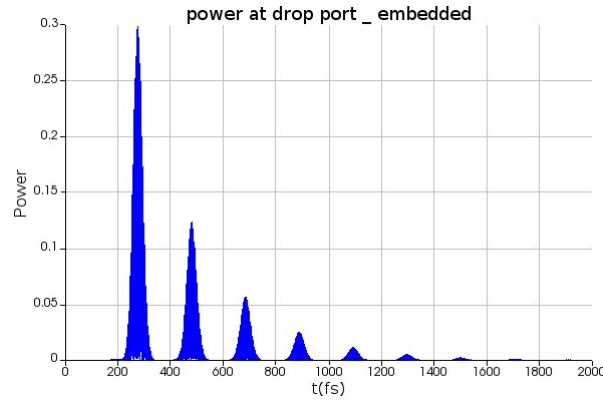


Figure 4.16: Power at the output port of embedded ring structure

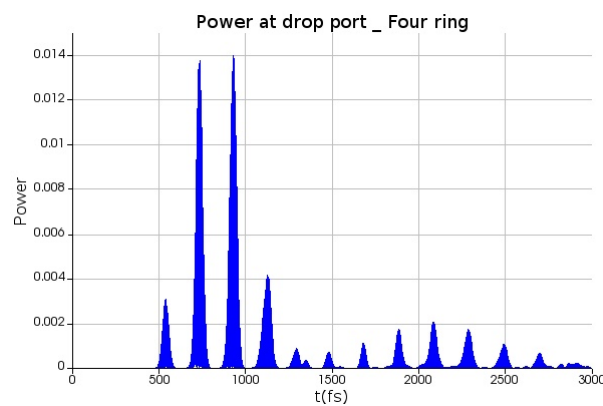


Figure 4.17: Power at the output port of four ring structure

4.1.2.2 Comparison between Four ring structure and interconnected ring structure

Also we can see that the power level has a detectable range for 750 fs in case of four ring structure. But in the case of interconnected structure the power level has a detectable range upto 1000 fs.

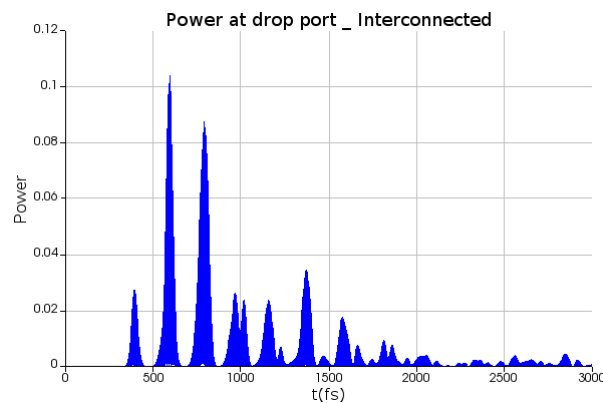


Figure 4.18: Power at the output port of interconnected structure

Table 4.2: Storage time and Power corresponding to the structures with different number of rings

| Structure | Storage time(fs) | Power(mW) |
|-----------------------|------------------|-------------|
| Single ring | 100 | 0.22 |
| Embedded | 100 | 0.31 |
| Two ring | 400 | 0.2 |
| Three ring | 490 | 0.034 |
| Four ring | 790 | 0.014 |
| Interconnected | 430 | 0.11 |

From Table 4.2 we can see that as the structure expands the storage time increases but power decreases. In the case of embedded structure, there is not as much difference in the case of storage time but there is a remarkable increase in case of power. When we look at the case of interconnected structure we can see that the power level is very large compared to four ring structure.

Chapter 5

Conclusion and Future scope

In today's digital environment, research on data transfer speed is crucial. The majority of data transfer today takes place across optical fibres, however when it comes to data processing applications, we must convert the data from light to electrical signals. The speed of data transfer will once more increase if we can avoid this conversion. Processing of the data should be done in the light form itself for that reason. Thus, light-based memory is the primary necessity. This work mainly focus on memory using micro ring resonator which store light energy.

In this work we simulated different micro ring resonator structures. Then we compare the storage time of light inside each structure.

According to the simulation results we find out that retention time of the light inside the structures mainly depends on the number of rings used and structural orientations of the rings. We observe that as the number of rings increases the retention time also increases, but the power at the output decreases when the rings are positioned parallel to one another. Another striking finding is that this power loss can be resolved when we use interconnected structures. Embedded structures will also aid in reducing power loss. Embedded structures will lessen the size of the overall structure in addition to lowering power loss. Taking into account all the observations, we came to a conclusion that micro ring resonator structures can be effectively used as data storage devices as it store light energy. Also the storage time can be increased by using interconnected and embedded ring structures.

This work can be extended by combining these structures. Here we use rings of same radius, but in future works we can use different radius rings at the same

structure. We can also use racetracks and square structures for analysis. No loss condition is analysed in this work, in future we can add different losses inside the structure.

Appendices

MRR - Micro Ring resonator

RAM - Random Access memory

WG - Waveguide

PC - Photonic Crystal

OADM - Optical Add or Drop Multiplexer

OCDF - Opticalchannel dropping filters

FWHM - Full Width Half Maximum

MRTEM - Micro ring

TMM - Transfer Matrix Method

FDTD - Finite Difference Time Doman

FSR - Free Spectral range

Q factor - Quality factor

References

- [1] T. Asano and S. Noda, “Ultra-high-Q photonic nanocavities and trapping of ultra-short optical pulses,” in Proc. Top. Meeting Slow Fast Light, Washington DC, 2006, p. MB41-2.
- [2] A. Rack, ”Optical delay line memory,” in IEEE Journal of Quantum Electronics, vol. 3, no. 6, pp. 246-246, June 1967, doi: 10.1109/JQE.1967.1074502.
- [3] J. M, Chen, Y. C., “Optical flip-flop”, Electronics Letters, vol. 21, pp. 236–238, 1985. doi:10.1049/el:19850169.
- [4] Kui, L.F., Uddin, M.R. “Photonic microring resonator modulated resonance response analysis”. Opt Quant Electron 49, 275 (2017). <https://doi.org/10.1007/s11082-017-1113-5>.
- [5] W. Hong, G. Gu, and Q. Chen, “Analysis of microring filter with two embedded microring,” Optik, vol. 124, pp. 3933–3935, Oct. (2013). <https://doi.org/10.1016/j.ijleo.2012.11.012>
- [6] Y. Xu, T. Liu, S. Liu, X. Sun and D. Zhang, ”Mutual-Coupling in High-Q Silicon Dual-Concentric Micro-Ring/Racetrack Resonator,” in IEEE Photonics Journal, vol. 14, no. 4, pp. 1-7, Aug. 2022, Art no. 6639707, <https://doi.org/10.1109/JPHOT.2022.3186914>
- [7]] Addya, S., Dey, S. Mandal, S. “Optical Ring Resonator Based Temperature Sensor.” Sens Imaging 18, 33 (2017). <https://doi.org/10.1007/s11220-017-0182-7>
- [8] Mamdouh, T., Khalil, D. “A MEMS Tunable Optical Ring Resonator Filter. ”Opt Quant Electron 37, 835–853 (2005). <https://doi.org/10.1007/s11082-005-0958-1>

- [9] C. -y. Chao, S. Ashkenazi, S. -w. Huang, M. O'Donnell and L. J. Guo, "High-frequency ultrasound sensors using polymer microring resonators," in *IEEE Transactions on Ultrasonics, Ferroelectrics, and Frequency Control*, vol. 54, no. 5, pp. 957-965, May 2007, <https://doi.org/10.1109/TUFFC.2007.341>.
- [10] D. Li, W. Chang, C. Liu, D. Liu and M. Zhang, "Broadband Wavelength Conversion Based on Parallel-Coupled Micro-Ring Resonators," in *IEEE Photonics Technology Letters*, vol. 30, no. 17, pp. 1559-1562, 1 Sept.1, 2018, doi: 10.1109/LPT.2018.2861753.
- [11] Rakshit, J.K., Roy, J.N. "Silicon micro-ring resonator-based all-optical digital-to-analog converter." *Photon Netw Commun* 34, 84–92 (2017). <https://doi.org/10.1007/s11107-016-0664-x>
- [12] Rakshit, J.K. "Design of Micro-ring Resonator Based 4×4 Optical Router for Photonic Network Applications." *Braz J Phys* 50, 582–593 (2020). <https://doi.org/10.1007/s13538-020-00767-6>
- [13] N. Moroney et al., "Logic Gates Based on Interaction of Counterpropagating Light in Microresonators," in *Journal of Lightwave Technology*, vol. 38, no. 6, pp. 1414-1419, 15 March15, 2020, doi: 10.1109/JLT.2020.2975119.
- [14] Law, F.K. et al., "Positive edge-triggered JK flip-flop using silicon-based micro-ring resonator." *Opt Quant Electron* 52, 314 (2020). <https://doi.org/10.1007/s11082-020-02432-3>
- [15] Bharti G.K et al., "Design of all-optical JK, SR and T flip-flops using micro-ring resonator-based optical switch." *Photon Netw Commun* 35, 381–391 (2018). <https://doi.org/10.1007/s11107-017-0754-4>
- [16] Law, F.K., Rakib Uddin, M., Hashim, H. et al. Demonstration of photonic micro-ring resonator based digital bit magnitude comparator. *Opt Quant Electron* 51, 1 (2019). <https://doi.org/10.1007/s11082-018-1712-9>
- [17] Kumar A et al., "Implementation of all-optical 1×4 memory register unit using the micro ring resonator structures." *Opt Quant Electron* 53, 492 (2021). <https://doi.org/10.1007/s11082-021-03131-3>

- [18] S. Tucker and J. L. Riding, "Optical Ring-Resonator Random-Access Memories," in *Journal of Lightwave Technology*, vol. 26, no. 3, pp. 320-328, Feb.1, 2008, doi: 10.1109/JLT.2007.909858